



HAL
open science

Miocene fire intensification linked to continuous aridification on the Tibetan Plateau

Yunfa Miao, Fuli Wu, Sophie Warny, Xiaomin Fang, Haijian Lu, Bihong Fu, Chunhui Song, Xiaoli Yan, Gilles Escarguel, Yibo Yan, et al.

► **To cite this version:**

Yunfa Miao, Fuli Wu, Sophie Warny, Xiaomin Fang, Haijian Lu, et al.. Miocene fire intensification linked to continuous aridification on the Tibetan Plateau. *Geology*, 2019, 47 (4), pp.303-307. 10.1130/G45720.1 . hal-02095433

HAL Id: hal-02095433

<https://univ-lyon1.hal.science/hal-02095433>

Submitted on 27 Feb 2024

HAL is a multi-disciplinary open access archive for the deposit and dissemination of scientific research documents, whether they are published or not. The documents may come from teaching and research institutions in France or abroad, or from public or private research centers.

L'archive ouverte pluridisciplinaire **HAL**, est destinée au dépôt et à la diffusion de documents scientifiques de niveau recherche, publiés ou non, émanant des établissements d'enseignement et de recherche français ou étrangers, des laboratoires publics ou privés.

Miocene fire intensification linked to continuous aridification on the Tibetan Plateau

Yunfa Miao^{1,2*}, Fuli Wu^{2*}, Sophie Warny³, Xiaomin Fang², Haijian Lu⁴, Bihong Fu⁵, Chunhui Song⁶, Xiaoli Yan⁶, Gilles Escarguel⁷, Yibo Yang², Qingquan Meng⁶, and Pilong Shi⁵

¹Key Laboratory of Desert and Desertification, Northwest Institute of Eco-Environment and Resources, Chinese Academy of Sciences, Lanzhou, China

²CAS Center for Excellence in Tibetan Plateau Earth Sciences and Key Laboratory of Continental Collision and Plateau Uplift,

Institute of Tibetan Plateau Research, Chinese Academy of Sciences, Beijing, China

³Department of Geology and Geophysics, and Museum of Natural Science, Louisiana State University, Baton Rouge, Louisiana, USA

⁴Institute of Geology, Chinese Academy of Geological Sciences, Beijing, China

⁵Institute of Remote Sensing and Digital Earth, Chinese Academy of Sciences, Beijing, China

⁶School of Earth Sciences, and Key Laboratory of Western China's Mineral Resources of Gansu Province, Lanzhou University, Lanzhou, China

⁷Laboratoire d'Ecologie des Hydrosystèmes Naturels et Anthropisés, UMR 5023 LEHNA, CNRS, ENTPE, Université Lyon 1, Villeurbanne, France

ABSTRACT

Although fire is considered an important factor in global vegetation evolution and climate change, few high-resolution Miocene fire records have been obtained worldwide. Here, two independent micro-charcoal-based fire records from the northern Tibetan Plateau were analyzed; both show similar trends in micro-charcoal concentrations through time, with low abundances in the warmer Middle Miocene Climate Optimum (18–14 Ma) followed by a continuous increase throughout the late Miocene (14–5 Ma) cooling. Our detailed statistical analyses show that the micro-charcoal concentration trend is highly positively correlated to the trend in oxygen isotopes ($\delta^{18}\text{O}$, $r = 0.94$) and xerophytic species ($\%_{\text{xero}}$, $r = 0.95$). We propose that the intensified fire frequency on the Tibetan Plateau mainly originated from the forest-steppe ecotone as a result of the continuous aridification in winter driven by the global cooling and decreased atmospheric $p\text{CO}_2$ that occurred during 18–5 Ma, with a secondary control by the tectonic activity of the northern Tibetan Plateau.

INTRODUCTION

Late Cenozoic global fire activity has been considered as one of the key factors influencing modern vegetation evolution and climate change (Bowman et al., 2009; Dale et al., 2001;

Edwards et al., 2010). However, globally, few Miocene high-resolution records have been obtained with which to assess fire occurrence (Hoetzel et al., 2013). As part of the second-largest arid to semi-arid area in the world, the northern Tibetan Plateau is a unique location for studying fire history, along with vegetation and aridity evolution (Miao et al., 2016); however, the region's numbers of fire records, sampling resolution, combustion source data, and controlling factors still need further investigation.

The charcoals resulting when plant matter is burned have been referred to as “fossils of fire” and are regarded as one of the most important proxies in the study of fire history (e.g., intensity, frequency, etc.) (Patterson et al., 1987; Whitlock and Larsen, 2002; Bowman et al., 2009; Bond, 2015). Here, we analyze fire histories based on relatively high-resolution micro-charcoal records from two independent sites on the northern Tibetan Plateau: the KC-1 core (38°03'N, 91°45'E; drilled by the Qinghai Petroleum Administration Bureau) in the Qaidam Basin, characteristic of a lacustrine environment (Miao et al., 2011), and the KM/KNX sections in the Kumkol Basin, characteristic of a fluvial-lacustrine environment (Lu et al., 2016, 2018) (Fig. 1).

STUDY SITES AND DATA

Situated in southern Inner Asia, the northern Tibetan Plateau is marked by a typical inland hyperarid climate, with mean annual

precipitation of <200 mm. As a result of its high elevation, the area is also very cold and windy. The Westerlies represent the dominant atmospheric circulation pattern throughout the year, while the East Asian summer monsoon generally reaches only the southeastern Qaidam Basin (Wu et al., 1985) (Fig. 1). Under these conditions, bare ridges and desert vegetation constitute the typical land cover. The desert vegetation that grows on gravelly lake margins and on well-drained soils of alluvial fans is composed mainly of *Ephedra*, *Nitraria*, *Tamarix*, Poaceae, Cyperaceae (as well as Asteraceae), and occasionally *Picea* and *Sabina* on the high mountains near the eastern part of the Qaidam Basin.

Tectonically, the ~1600-km-long Altyn Tagh fault separates the low-lying Tarim Basin to the north from the Tibetan Plateau. The left-lateral strike-slip Kunlun fault marks the northern boundary of the high-elevation, low-relief main part of the Tibetan Plateau, extending for ~1500 km. A broad triangular area consisting of the Kumkol Basin, the Qiman Tagh range, and the Qaidam Basin is bounded to the northwest by the Altyn Tagh fault and to the south by the Kunlun fault (Fig. 1). Previous work based on apatite fission-track modeling has shown that the Qaidam and Kumkol Basins have been separated by the synchronous initial uplift of Qiman Tagh at ca. 40–30 Ma (Liu et al., 2017).

The present Qaidam Basin, with an average elevation of ~3000 m, is the largest intermontane basin on the northeastern Tibetan Plateau, and

*E-mails: miaoyunfa@lzb.ac.cn; wufuli@itpcas.ac.cn

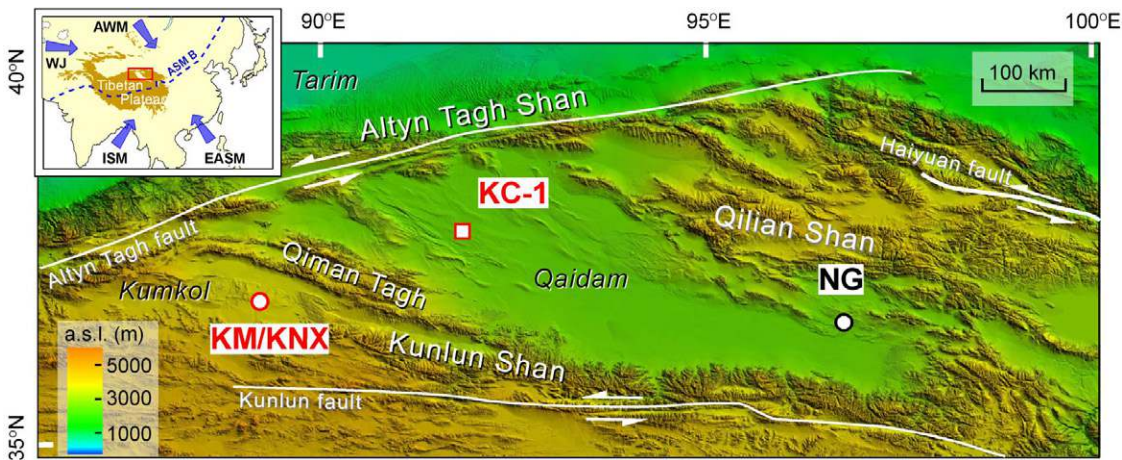


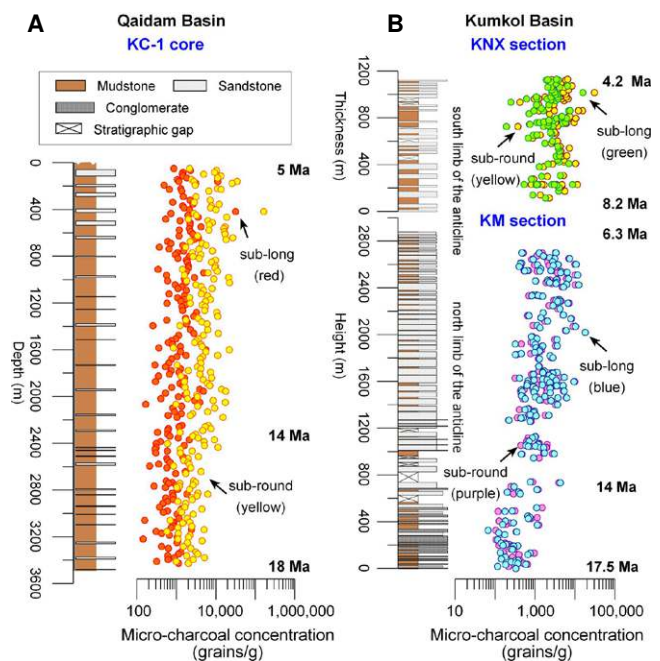
Figure 1. Location map showing northern Tibetan Plateau, major strike-slip faults, and sites of micro-charcoal study. KM/KNX sections and KC-1 core are located in the Kumkol and western Qaidam Basins, respectively. NG section lies in the eastern Qaidam Basin (Miao et al., 2016). AWM—Asian winter monsoon; ASM B—Asian summer monsoon boundary; EASM—East Asian summer monsoon; ISM—Indian summer monsoon; WJ—Westerly jet.

covers an area of ~120,000 km². The sediments recovered from the KC-1 core, reaching 3425 m in depth, were extracted from the western basin and span ages of 18 Ma to 5 Ma, with an average sedimentation rate of ~260 m/m.y. (Miao et al., 2011) (Fig. 2A). Another section, named NG (Naoge), from the eastern basin and spanning ages of ca. 18–10 Ma, was also used for comparison (for details, see Miao et al., 2016). The rhombus-shaped Kumkol Basin has an average elevation of ~4200 m and an area of ~17,500 km² (Fig. 1). We sampled the KM section, spanning 2869 m in thickness, and the KNX section, spanning 1125 m, from the central basin. Chronostratigraphic analysis of these two sections yielded ages of 17.5–6.3 Ma in the KM section (Lu et al., 2016), and 8.2–4.2 Ma in the KNX section (Lu et al., 2018), providing average sedimentation rates of ~260 m/m.y. and ~290 m/m.y., respectively (Fig. 2B). The composite age range of 17.5–5.0 Ma for these two sections (herein KM/KNX) was used for the micro-charcoal analyses and comparison with the KC-1 core.

METHODS AND RESULTS

In this study, 188 samples from the KC-1 core (Qaidam Basin) and 250 samples from the KM/KNX sections (Kumkol Basin) were used for micro-charcoal identification and processed via standard palynological techniques. A known number of *Lycopodium clavatum* spores were initially added to each sample for calculating the micro-charcoal concentration (MC) (Miao et al., 2016). Two basic micro-charcoal shapes (sub-long [*L*] and sub-round [*R*]) were identified by calculating the ratio of length (major axis) to width (minor axis): if the value was >2.5, the micro-charcoal grain was classified as *L*, and if <2.5, as *R*. The MCs for both types (MC_L and MC_R, respectively) were determined, and then added together to obtain the total MC values, referred to as MC_{total} (Table DR4 in the GSA Data Repository¹). The MC_{total} for the previously

Figure 2. Micro-charcoal records and lithology (see Fig. 1 for location). A: KC-1 core, western Qaidam Basin, northern Tibetan Plateau, dominated by lacustrine sediments. B: Composite KM and KNX sections, Kumkol Basin, dominated by fluvial-lacustrine sediments. Colored dots indicate micro-charcoal concentration (MC), in grains per gram; subscripts *L* and *R* refer to sub-long and sub-round grains, respectively.



studied NG section in the eastern Qaidam Basin (Miao et al., 2016; Fig. 1) was also included in the statistical analyses.

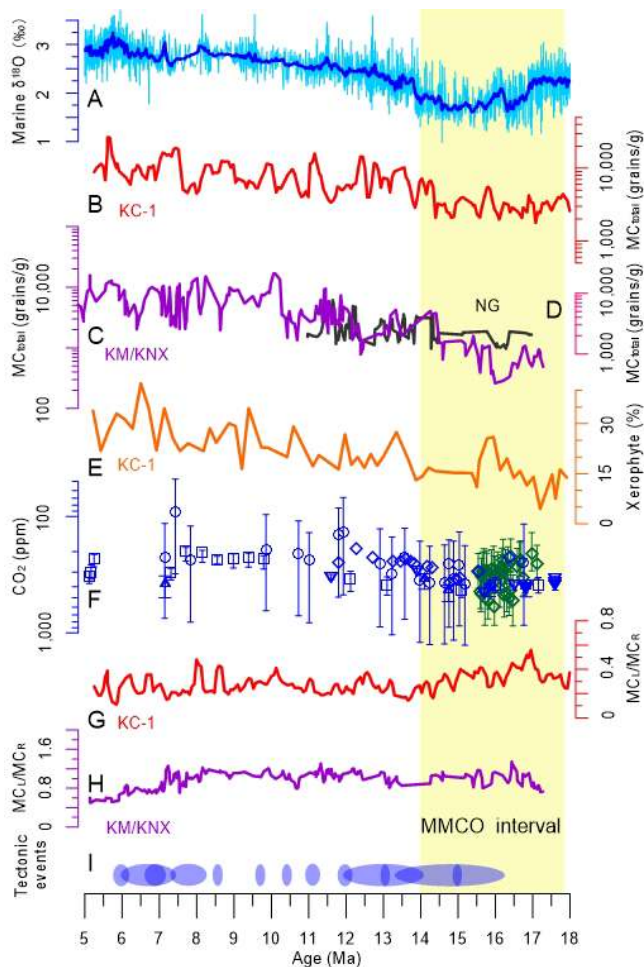
First, the existence of a trend in the three separate time series (KC-1, KM/KNX, and NG) of observed MC_{total} values was tested using the Mann-Kendall trend test (Table DR1). Then Pearson correlations were computed for the three possible pairs of MC_{total} time series based on spline-fitted log-transformed MC_{total} values interpolated every 50 k.y. along each time series, resulting in three interpolated data sets described within the same time frame (Table DR2). Last, a composite MC_{total} time series was compiled from the three separate series, and finally correlated to the time series of marine δ¹⁸O, atmospheric pCO₂, and percentages of xerophytic taxa in the Qaidam Basin using the same interpolation procedure based on spline-fitted curves (Table

DR3). In all cases, correlation significance was evaluated through a Mantel test based either on the interpolated MC_{total} values or on the time autocorrelation-free first-order differences between “raw” interpolated MC_{total} values. All computations were done using PAST software, version 3.16 (<https://folk.uio.no/ohammer/past/>; Hammer et al., 2001).

The most notable characteristics between the KC-1 and KM/KNX sites are their similar patterns (Pearson *r* = 0.95; Table DR2) but different absolute values of MC_R, MC_L, and MC_{total}. The KC-1 core has the highest grain counts, varying between 46,300 and 900 grains/g, with an average of ~7000 grains/g (Fig. 2A). The KM/KNX sections vary between 36,100 and 200 grains/g, with an average of ~4000 grains/g (Fig. 2B). Overall, the trends of MC_{total} in the three sections (including NG) are all highly significantly increasing with time (Figs. 3B–3D; Tables DR1 and DR2). As a result, the composite MC_{total} time series also shows a highly significant trend (Mann-Kendall

¹GSA Data Repository item 2019105, micro-charcoal data and details of the statistical analyses, is available online at <http://www.geosociety.org/datarepository/2019/>, or on request from editing@geosociety.org.

Figure 3. Data time series of climatic proxies and tectonic events on the northern Tibetan Plateau. MMCO—Middle Miocene Climate Optimum. A: Global deep-sea $\delta^{18}\text{O}$ records (Zachos et al., 2001) (light blue) with 12-point averaging (darker blue). B–D: Micro-charcoal concentration (MC) records from KC-1 core, western Qaidam Basin (this study) (B), KM/KNX sections, Kumkol Basin (this study) (C), and NG section, eastern Qaidam Basin (Miao et al., 2016) (D). E: Xerophytic pollen percentages in KC-1 core (Miao et al., 2011). F: Synthesis of published $p\text{CO}_2$ proxy data. Boron (diamonds) from Foster et al., 2012; Greenop et al., 2014. Stomata (inverted triangles) from Kürschner et al., 2008. Alkenone (regular triangles) from Zhang et al., 2013. B/Ca (squares) from Tripathi et al., 2009. Paleosol (circles) from Ji et al., 2018. Error bars represent uncertainties in underlying assumptions of each proxy. G,H: Ratios of MC_L/MC_R (L —sub-long grains; R —sub-round grains) from KC-1 core and KM/KNX sections, respectively (this study). I: Tectonic events on the northern Tibetan Plateau (after Miao et al. [2012], Li et al. [2014], and Chang et al. [2015]). Curves in B–D and G–H are by three-point averaging.



test: $S = 54,543$; $Z = 11.88$; $p = 1.5 \times 10^{-32}$) corresponding to an increase of approximately one order of magnitude in the spline-fitted MC_{total} curve over the analyzed time interval. This composite spline-fitted MC_{total} curve shows a very high correlation ($r = 0.94$) with the global deep-sea isotope record at a 50 k.y. time resolution (Zachos et al., 2001) (Fig. 3A; Table DR3). Additionally, it also highly correlates ($r = 0.95$) with the xerophytic pollen abundances in the KC-1 core (*Ephedra*, *Nitraria*, Chenopodiaceae (Amaranthaceae), *Artemisia* and other Asteraceae taxa, etc.; Miao et al., 2011; Fig. 3E), whereas it is negatively correlated ($r = -0.86$) to the comprehensive $p\text{CO}_2$ record (Kürschner et al., 2008; Tripathi et al., 2009; Foster et al., 2012; Greenop et al., 2014; Ji et al., 2018; Fig. 3F).

DISCUSSION

Fire and Aridification

Based on the relationship between MC_{total} and fire (Hoetzel et al., 2013; Patterson et al., 1987; Bond, 2015), higher values of MC_{total} over long time scales (e.g., millions of years) can be related to increased fire activity, e.g., greater

frequency or intensity. The MC_{total} data from the KC-1 core and KM/KNX sections (Figs. 3B and 3C), as well as from the NG section (Miao et al., 2016) (Fig. 3D), support the view that fire activity on the northern Tibetan Plateau steadily increased during the middle to late Miocene. The overall average expansion of xerophytic vegetation in the western Qaidam Basin (Miao et al., 2011), as well as an increase in MC_{total} , support an increase in fire activity and suggest that these two phenomena are strongly linked from 18 to 5 Ma (Miao et al., 2016). A relatively low fire frequency and/or strength occurred during the relatively wet Middle Miocene Climate Optimum (MMCO, 18–14 Ma), while an overall increasing trend is observed during the drier late Miocene (14–5 Ma).

Fire Distribution

Although the relationship between fire intensification and aridification on the northern Tibetan Plateau correlates well, the question of fire distribution remains. It is very important to understand whether the fire intensification is due to an enlarged combustion area or an increase of combustion frequencies.

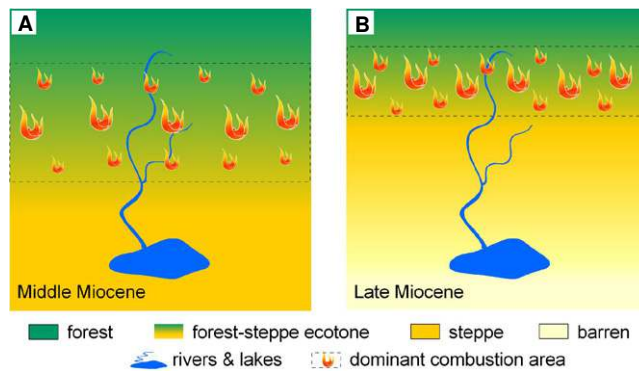
Studies show that the L and R in micro-charcoal shapes represent grass and wood sources, respectively (Umbanhowar and Mcgrath, 1998; Daniau et al., 2013; Crawford and Belcher, 2014). This means that the samples with higher MC_L seem to be dominated by the combustion of grasses, while the samples with higher MC_R seem to be dominated by combustion of wood. Therefore, the ratios of MC_L/MC_R can be directly used to indicate the grass/wood ratios during combustion, with higher values indicating more grass than wood, and vice versa. In this study, the higher values of the MC_L/MC_R in the KM/KNX sections (~ 0.6 – 1.0) are related to combustion dominated by grass (Fig. 3H), while lower values in the KC-1 core (~ 0 – 0.5) suggest relatively higher wood combustion (Fig. 3G). Interestingly, although the MC_L/MC_R values are different, the trends remained stable over the examined interval for both sections. Therefore, despite differences in vegetation source material between the two sections, and the expansion of grasslands during late Miocene cooling, the forest-steppe ecotone must have still been the dominant environment where fire occurred in order for such stable trends in MC_L/MC_R values to have been maintained. The conceptual renderings in Figure 4 illustrate this phenomenon. During the MMCO, the area of the forest-steppe ecotone was large but fire frequency was low (Fig. 4A) under the relatively wet climate (Miao et al., 2011), and less micro-charcoals were produced (Fig. 4A). In contrast, during the late Miocene, the forest-steppe ecotone remained a fire source area but likely experienced an overall decreasing trend in areal extent as xerophytic vegetation expanded under a drying climate (Miao et al., 2011). However, the persistently increasing fire frequency due to the drier conditions produced more charcoal particles, thereby greatly counteracting the negative effect of ecotone shrinkage (Fig. 4B).

Global Cooling, CO_2 , and Tectonics

After compiling global low-sampling-resolution fire records, Bond (2015) argued that none of the potential global factors (oxygen, rainfall seasonality, CO_2 , novel flammable growth forms) could adequately explain the spread of increased fire activity over long Cenozoic time scales. In this study, the increasing fire frequency is strongly negatively correlated to Bond's compiled results of atmospheric $p\text{CO}_2$ ($r = -0.86$; Fig. 3F) and is positively closely linked to the global oxygen isotope record (Zachos et al., 2001) ($r = 0.94$; Fig. 3A) and the expansion of xerophytic vegetation ($r = 0.95$; Miao et al., 2011; Fig. 3E).

CO_2 has been argued as having an important role in fertilization of vegetation through affecting photosynthetic assimilation (Wolfe and Erickson, 1993), thus changing the amount of annual gross primary production (Sun et al., 2014). Theoretically, high $p\text{CO}_2$ facilitates

Figure 4. Conceptual diagram showing change in fire location on the northern Tibetan Plateau in relation to xerophytic vegetation expansion. A: During warm and wet Middle Miocene, e.g., Middle Miocene Climate Optimum, area experiencing fires was large, but fire frequency was low, causing total micro-charcoal concentration (MC_{total}) to be low. B: During late Miocene cooling and drying, area with fire activity shrank but fire frequency became much higher, causing MC_{total} to steadily increase. In both A and B, fire mainly occurred in forest-steppe ecotone to keep MC_L/MC_R (L —sub-long grains; R —sub-round grains) ratio broadly stable.



regional vegetation biomass, which, as a result, provides an underlying source for higher MC during combustion, and vice versa. However, the negative correlation between CO_2 and MC may indicate a complicated relationship between pCO_2 and MC.

Global cooling can also be argued as having a major role on the fire through reducing the amount of water vapor held in the atmosphere, favoring drier vegetation (Miao et al., 2012) and, ultimately, increasing combustion frequencies. But the relationship is not always that simple, and seasonal variability has to be taken under consideration. For instance, taking into account the magnetic proxy built up in the Qaidam Basin possibly indicating a wetting event driven by the East Asian summer monsoon at 8.2–7.8 Ma (Nie et al., 2017), we argue that the wet-dry monsoonal climate might have played a major role in promoting fires during the late Miocene. Grasses grow in the wet season and become highly flammable in the dry season; that is, the drier trends most possibly occurred in the winter.

While it is intuitive to link global cooling to increased fire via the role of aridification (Miao et al., 2012), uplift of the Tibetan Plateau has been argued as the primary driver of global cooling and atmospheric pCO_2 decline (Raymo and Ruddiman, 1992; France-Lanord and Derry, 1997; Kump et al., 2000; Galy et al., 2015), which means that fire frequency should have also been clearly increased by the uplift of the Tibetan Plateau, possibly as much as by the atmospheric pCO_2 change. In fact, the uplift of the northeastern Tibetan Plateau is also viewed as a potentially important factor controlling regional aridification (Zhuang et al., 2011; Liu et al., 2015). However, the uplift process is characterized by multiple-stage pulses with enhanced uplift at ca. 15 Ma (Chang et al., 2015), ca. 12 Ma (Wang et al., 2017), and ca. 8 Ma (Fang et al., 2007; Li et al., 2014) (Fig. 3I). The continuous fire intensification has not shown obvious responses to these rapid uplift periods, implying that regional uplift might not be the primary factor controlling fire activity.

CONCLUSION

A series of detailed micro-charcoal data sets obtained from two new independent sites on the northern Tibetan Plateau (from the KC-1 core in the western Qaidam Basin) and previously published data from the NG section in the eastern Qaidam Basin, offer a perspective on the fire history during 18–5 Ma on the northern Tibetan Plateau. Our results show increased fire occurrence based on low values of micro-charcoal during the warm and less-dry MMCO to high values during the cooler and drier late Miocene. Increased fire frequencies in the forest-steppe ecotone counterbalanced the concurrent reduction in combustion area. Our data and statistical analyses support the view that fire activity on the northern Tibetan Plateau is primarily linked to global cooling, with decreased atmospheric pCO_2 reflecting the continuous aridification on the northern Tibetan Plateau at 18–5 Ma. The influence of tectonic activity on the northern Tibetan Plateau is likely a secondary controlling factor.

ACKNOWLEDGMENTS

We thank the anonymous reviewers, whose comments greatly improved the quality of the manuscript. We are grateful to Y.D. Duan, Y.H. Miao, and F.Z. Zhang for assistance in the laboratory. This work was co-supported by: the Strategic Priority Research Program of the Chinese Academy of Sciences (CAS): (grants XDA20070202 and 20070201); the Second Tibetan Plateau Scientific Expedition Program (STEP); the National Natural Science Foundation of China (grants 41772181, 41620104002, 41872098); the National Science Foundation of Gansu Province (grant 18JR3RA395); the Member of Youth Innovation Promotion Association (grant 2014383); and the “Light of West China” Program and State Key Laboratory of Loess and Quaternary Geology, Institute of Earth Environment, CAS (grant SKLLQG1515).

REFERENCES CITED

Bond, W.J., 2015, Fires in the Cenozoic: A late flowering of flammable ecosystems: *Frontiers of Plant Science*, v. 5, 749, <https://doi.org/10.3389/fpls.2014.00749>.

Bowman, D.M., Balch, J.K., Artaxo, P., Bond, W.J., Carlson, J.M., Cochrane, M.A., D’Antonio, C.M.,

DeFries, R.S., Doyle, J.C., and Harrison, S.P., 2009, Fire in the Earth system: *Science*, v. 324, p. 481–484, <https://doi.org/10.1126/science.1163886>.

- Chang, H., Li, L., Qiang, X., Garzzone, C.N., Pullen, A., and An, Z., 2015, Magnetostratigraphy of Cenozoic deposits in the western Qaidam Basin and its implication for the surface uplift of the northeastern margin of the Tibetan Plateau: *Earth and Planetary Science Letters*, v. 430, p. 271–283, <https://doi.org/10.1016/j.epsl.2015.08.029>.
- Crawford, A.J., and Belcher, C.M., 2014, Charcoal morphometry for paleoecological analysis: The effects of fuel type and transportation on morphological parameters: *Applications in Plant Sciences*, v. 2, 1400004, <https://doi.org/10.3732/apps.1400004>.
- Dale, V.H., Joyce, L.A., McNulty, S., Neilson, R.P., Ayres, M.P., Flannigan, M.D., Hanson, P.J., Irland, L.C., Lugo, A.E., and Peterson, C.J., 2001, Climate change and forest disturbances: Climate change can affect forests by altering the frequency, intensity, duration, and timing of fire, drought, introduced species, insect and pathogen outbreaks, hurricanes, windstorms, ice storms, or landslides: *Bioscience*, v. 51, p. 723–734, [https://doi.org/10.1641/0006-3568\(2001\)051\[0723:CCAFD\]2.0.CO;2](https://doi.org/10.1641/0006-3568(2001)051[0723:CCAFD]2.0.CO;2).
- Daniau, A.L., Goñi, M.F.S., Martinez, P., Urrego, D.H., Bout-Roumzeilles, V., Desprat, S., and Marlon, J.R., 2013, Orbital-scale climate forcing of grassland burning in southern Africa: *Proceedings of the National Academy of Sciences of the United States of America*, v. 110, p. 5069–5073, <https://doi.org/10.1073/pnas.1214292110>.
- Edwards, E.J., Osborne, C.P., Strömberg, C.A., Smith, S.A., and the C₄ Grasses Consortium, 2010, The origins of C₄ grasslands: Integrating evolutionary and ecosystem science: *Science*, v. 328, p. 587–591, <https://doi.org/10.1126/science.1177216>.
- Fang, X., Zhang, W., Meng, Q., Gao, J., Wang, X., King, J., Song, C., Dai, S., and Miao, Y., 2007, High-resolution magnetostratigraphy of the Neogene Huaitoutala section in the eastern Qaidam Basin on the NE Tibetan Plateau, Qinghai Province, China and its implication on tectonic uplift of the NE Tibetan Plateau: *Earth and Planetary Science Letters*, v. 258, p. 293–306, <https://doi.org/10.1016/j.epsl.2007.03.042>.
- Foster, G.L., Lear, C.H., and Rae, J.W., 2012, The evolution of pCO_2 , ice volume and climate during the middle Miocene: *Earth and Planetary Science Letters*, v. 341, p. 243–254, <https://doi.org/10.1016/j.epsl.2012.06.007>.
- France-Lanord, C., and Derry, L.A., 1997, Organic carbon burial forcing of the carbon cycle from Himalayan erosion: *Nature*, v. 390, p. 65–67, <https://doi.org/10.1038/36324>.
- Galy, V., Peucker-Ehrenbrink, B., and Eglinton, T., 2015, Global carbon export from the terrestrial biosphere controlled by erosion: *Nature*, v. 521, p. 204–207, <https://doi.org/10.1038/nature14400>.
- Greenop, R., Foster, G.L., Wilson, P.A., and Lear, C.H., 2014, Middle Miocene climate instability associated with high-amplitude CO_2 variability: *Paleoceanography and Paleoclimatology*, v. 29, p. 845–853, <https://doi.org/10.1002/2014PA002653>.
- Hammer, Ø., Harper, D.A.T., and Ryan, P.D., 2001, PAST: Paleontological statistics software package for education and data analysis: *Palaeontologia Electronica*, v. 4, 4.
- Hoetzel, S., Dupont, L., Schefuß, E., Rommelskirchen, F., and Wefer, G., 2013, The role of fire in Miocene to Pliocene C₄ grassland and ecosystem evolution: *Nature Geoscience*, v. 6, p. 1027–1030, <https://doi.org/10.1038/ngeo1984>.

- Ji, S., Nie, J., Lechler, A., Huntington, K.W., Heitmann, E.O., and Breecker, D.O., 2018, A symmetrical CO₂ peak and asymmetrical climate change during the middle Miocene: *Earth and Planetary Science Letters*, v. 499, p. 134–144, <https://doi.org/10.1016/j.epsl.2018.07.011>.
- Kump, L.R., Brantley, S.L., and Arthur, M.A., 2000, Chemical weathering, atmospheric CO₂, and climate: *Annual Review of Earth and Planetary Sciences*, v. 28, p. 611–667, <https://doi.org/10.1146/annurev.earth.28.1.611>.
- Kürschner, W.M., Kvaček, Z., and Dilcher, D.L., 2008, The impact of Miocene atmospheric carbon dioxide fluctuations on climate and the evolution of terrestrial ecosystems: *Proceedings of the National Academy of Sciences of the United States of America*, v. 105, p. 449–453, <https://doi.org/10.1073/pnas.0708588105>.
- Li, J., Fang, X., Song, C., Pan, B., Ma, Y., and Yan, M., 2014, Late Miocene–Quaternary rapid stepwise uplift of the NE Tibetan Plateau and its effects on climatic and environmental changes: *Quaternary Research*, v. 81, p. 400–423, <https://doi.org/10.1016/j.yqres.2014.01.002>.
- Liu, D., Li, H., Sun, Z., Pan, J., Wang, M., and Wang, H., 2017, AFT dating constrains the Cenozoic uplift of the Qimen Tagh Mountains, Northeast Tibetan Plateau, comparison with LA-ICPMS Zircon U–Pb ages: *Gondwana Research*, v. 41, p. 438–450, <https://doi.org/10.1016/j.gr.2015.10.008>.
- Liu, X., Sun, H., Miao, Y., Dong, B., and Yin, Z.-Y., 2015, Impacts of uplift of northern Tibetan Plateau and formation of Asian inland deserts on regional climate and environment: *Quaternary Science Reviews*, v. 116, p. 1–14, <https://doi.org/10.1016/j.quascirev.2015.03.010>.
- Lu, H., Fu, B., Shi, P., Ma, Y., and Li, H., 2016, Constraints on the uplift mechanism of northern Tibet: *Earth and Planetary Science Letters*, v. 453, p. 108–118, <https://doi.org/10.1016/j.epsl.2016.08.010>.
- Lu, H., Fu, B., Shi, P., Xue, G., and Li, H., 2018, Late-Miocene thrust fault-related folding in the northern Tibetan Plateau: Insight from paleomagnetic and structural analyses of the Kumkol basin: *Journal of Asian Earth Sciences*, v. 156, p. 246–255, <https://doi.org/10.1016/j.jseas.2018.01.026>.
- Miao, Y., Fang, X., Herrmann, M., Wu, F., Zhang, Y., and Liu, D., 2011, Miocene pollen record of KC-1 core in the Qaidam Basin, NE Tibetan Plateau and implications for evolution of the East Asian monsoon: *Palaeogeography, Palaeoclimatology, Palaeoecology*, v. 299, p. 30–38, <https://doi.org/10.1016/j.palaeo.2010.10.026>.
- Miao, Y., Herrmann, M., Wu, F., Yan, X., and Yang, S., 2012, What controlled Mid–Late Miocene long-term aridification in Central Asia?—Global cooling or Tibetan Plateau uplift: A review: *Earth-Science Reviews*, v. 112, p. 155–172, <https://doi.org/10.1016/j.earscirev.2012.02.003>.
- Miao, Y., Fang, X., Song, C., Yan, X., Zhang, P., Meng, Q., Li, F., Wu, F., Yang, S., and Kang, S., 2016, Late Cenozoic fire enhancement response to aridification in mid-latitude Asia: Evidence from microcharcoal records: *Quaternary Science Reviews*, v. 139, p. 53–66, <https://doi.org/10.1016/j.quascirev.2016.02.030>.
- Nie, J., Garzzone, C., Su, Q., Liu, Q., Zhang, R., Heslop, D., Necula, C., Zhang, S., Song, Y., and Luo, Z., 2017, Dominant 100,000-year precipitation cyclicity in a late Miocene lake from northeast Tibet: *Science Advances*, v. 3, e1600762.
- Patterson, W.A., III, Edwards, K.J., and Maguire, D.J., 1987, Microscopic charcoal as a fossil indicator of fire: *Quaternary Science Reviews*, v. 6, p. 3–23, [https://doi.org/10.1016/0277-3791\(87\)90012-6](https://doi.org/10.1016/0277-3791(87)90012-6).
- Raymo, M.E., and Ruddiman, W.F., 1992, Tectonic forcing of late Cenozoic climate: *Nature*, v. 359, p. 117–122, <https://doi.org/10.1038/359117a0>.
- Sun, Y., Gu, L., Dickinson, R.E., Norby, R.J., Pallardy, S.G., and Hoffman, F.M., 2014, Impact of mesophyll diffusion on estimated global land CO₂ fertilization: *Proceedings of the National Academy of Sciences of the United States of America*, v. 111, p. 15,774–15,779, <https://doi.org/10.1073/pnas.1418075111>.
- Tripati, A.K., Roberts, C.D., and Eagle, R.A., 2009, Coupling of CO₂ and ice sheet stability over major climate transitions of the last 20 million years: *Science*, v. 326, p. 1394–1397, <https://doi.org/10.1126/science.1178296>.
- Umbanhowar, C.E., Jr., and Mcgrath, M.J., 1998, Experimental production and analysis of microscopic charcoal from wood, leaves and grasses: *The Holocene*, v. 8, p. 341–346, <https://doi.org/10.1191/095968398666496051>.
- Wang, W., et al., 2017, Expansion of the Tibetan Plateau during the Neogene: *Nature Communications*, v. 8, 15887, <https://doi.org/10.1038/ncomms15887>.
- Whitlock, C., and Larsen, C., 2002, Charcoal as a fire proxy, in Smol, J.P., et al., eds., *Tracking Environmental Change using Lake Sediments*: Dordrecht, Springer, *Developments in Paleoenvironmental Research*, v. 3, p. 75–97, https://doi.org/10.1007/0-306-47668-1_5.
- Wolfe, D.W., and Erickson, J.D., 1993, Carbon dioxide effects on plants: Uncertainties and implications for modeling crop response to climate change, in Kaiser, H.M., and Drennen, T.E., eds., *Agricultural Dimensions of Global Climate Change*: Delray Beach, Florida, St. Lucie Press, p. 153–178.
- Wu, G.H., Hu, S.X., Zhang, Z.L., Zhao, H., and Fang, X., 1985, The Qaidam basin: *Journal of Lanzhou University*, v. 21, p. 35–52 (in Chinese).
- Zachos, J., Pagani, M., Sloan, L., Thomas, E., and Billups, K., 2001, Trends, rhythms, and aberrations in global climate 65 Ma to present: *Science*, v. 292, p. 686–693, <https://doi.org/10.1126/science.1059412>.
- Zhang, Y.G., Pagani, M., Liu, Z., Bohaty, S.M., and DeConto, R., 2013, A 40-million-year history of atmospheric CO₂: *Philosophical Transactions of the Royal Society A*, v. 371, 20130096, <https://doi.org/10.1098/rsta.2013.0096>.
- Zhuang, G., Hourigan, J.K., Koch, P.L., Ritts, B.D., and Kent-Corson, M.L., 2011, Isotopic constraints on intensified aridity in Central Asia around 12 Ma: *Earth and Planetary Science Letters*, v. 312, p. 152–163, <https://doi.org/10.1016/j.epsl.2011.10.005>.